

Chemically-exfoliated single-layer MoS₂ : stability, lattice dynamics and catalytic adsorption from first principles

Matteo Calandra*

Université Pierre et Marie Curie, IMPMC, CNRS UMR7590, 4 Place Jussieu, 75005 Paris, France

Chemically and mechanically exfoliated MoS₂ single-layer samples have substantially different properties. While mechanically exfoliated single-layers are mono-phase (1H polytype with Mo in trigonal prismatic coordination), the chemically exfoliated samples show coexistence of three different phases, 1H, 1T (Mo in octahedral coordination) and 1T' (a distorted 2 × 1 1T-superstructure). By using first-principles calculations, we investigate the energetics and the dynamical stability of the three phases. We show that the 1H phase is the most stable one, while the metallic 1T phase, strongly unstable, undergoes a phase transition towards a metastable and insulating 1T' structure composed of separated zig-zag chains. We calculate electronic structure, phonon dispersion, Raman frequencies and intensities for the 1T' structure. We provide a microscopical description of the J₁, J₂ and J₃ Raman features first detected more than 20 years ago, but unexplained up to now. Finally, we show that H adsorbates, that are naturally present at the end of the chemical exfoliation process, stabilize the 1T' over the 1H one.

I. INTRODUCTION

Bulk transition metal dichalcogenides (TMD) are layered van der Waals solids displaying remarkable properties promising both for fundamental research as well as for technological applications. Metallic bulk transition metal dichalcogenides (TMD) like NbSe₂, present coexistence of charge density wave and superconductivity^{1,2}, while insulating TMD (MoS₂, WS₂) are flexible, have high mobilities and are routinely used in flexible electronics.

Since the pioneering work of Frindt and coworkers³⁻⁶ and the successive developments in the fields of mechanical⁷ and liquid⁸ exfoliation, it has been possible to obtain free-standing or supported single-layer TMD. These monolayers are the inorganic analogue of graphene and display a rich chemistry⁹ that makes them attractive for energy storage applications. Insulating single-layer TMD have much lower mobilities^{10,11} than Graphene, but are nevertheless interesting for nanoelectronics, mainly due to the presence of a finite bandgap.

In this context, MoS₂ is considered one of the most promising materials¹². The most stable polytype of bulk MoS₂ is the 2H (Molybdenite), where each Mo has a trigonal prismatic coordination with the nearby S atoms. Mechanical exfoliation of bulk 2H MoS₂ lead to formation of single layer samples with the same local coordination (here labeled 1HMoS₂). In chemically exfoliated samples the situation is different. In the first step of chemical exfoliation of bulk 2H MoS₂, Li atoms are intercalated between the layers. The Li intercalation stabilize a 1T Li_xMoS₂ polytype having each Mo octahedrally coordinated with the nearby S atoms. Subsequent hydration with excess water and ultrasonication leads to the separation of the layers via LiOH formation and synthesis of large-area single-layer MoS₂ samples⁴.

The properties of chemically exfoliated MoS₂ single layers are poorly understood. Recently it has been shown that these samples are actually composed of heterostruc-

tures of 1H, 1T and 1T-distorted (labeled 1T') MoS₂ phases¹³. The 1T' phase is a 2 × 1 superstructure of the 1T phase formed by zig-zag chains. Remarkably, the three phases coexist in the same sample and have substantially different conducting properties as the 1T phase is metallic while the 1H and 1T' are insulating¹⁴. Upon mild annealing at 200 – 300 C the 1T and 1T' phase disappear and transform in the 1H one. Exposure to a 60 – 80 keV electron beam induces S vacancies¹⁵ and transforms the 1T' phase into the 1T one^{13,16}. Finally, it is important to remark that chemically exfoliated single layers are covered with adsorbates that can play some role in stabilizing one structure or the other.

The dynamical properties of the 1T' phase are not understood. For example, while it is well established that the high energy optical Raman spectra of the 1H phase are composed of two prominent peaks, attributed to the E_{2g} mode at ≈ 385 cm⁻¹ and to the A_{1g} mode at ≈ 403 cm⁻¹¹⁷, little is known on the Raman spectra of the 1T' phase. Raman measurements¹⁸ on freshly-prepared single-layers with dominant 1T' phase show that the E_{2g} peak is missing, while at least five additional peaks appear at lower energies (some of these peaks are labeled J₁, J₂, J₃). Nothing is known on the phonon displacements generating these features.

In this work we study the stability, the electronic structure and the dynamical properties of the 1T and 1T' phases in single layer MoS₂ by using density functional theory (DFT) calculations. We show that the metallic 1T phase is dynamically unstable. We find distorted structures with a 2 × 1 (1T' MoS₂) and 2 × 2 (labeled 1T'' MoS₂) real space periodicities having lower energies than the 1T one. Both 1T' and 1T'' structures are, however, substantially higher in energy than the 1HMoS₂ phase (see Fig.1 for a plot of the crystal structure of the different phases).

We then fully characterize the distorted 1T' phase found in experiments on chemically exfoliated MoS₂, by obtaining its electronic structure, phonon dispersion and Raman intensities. Finally, we study catalytic absorption

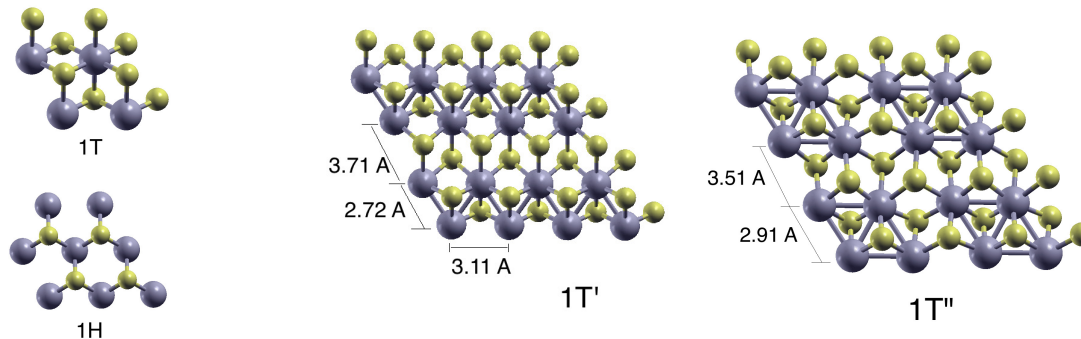


FIG. 1: Phases of chemically exfoliated MoS₂. The 1H has trigonal prismatic coordination and is the most stable among all polytypes. The 1T, 1T' and 1T'' polytypes all have octahedral coordination. The 1T' is the lowest energy polytype among those with octahedral coordination. The in-plane Mo-Mo distance is 3.193 Å and 3.183 Å for the 1T' and 1H structures, respectively

in the 1T' phase and show that H adsorbates stabilize the 1T' with respect to all the others.

The paper is organised as follows. In section II we describe the technical details of the calculation. In sec. III A we analyze the stability of octahedral phases with respect to the trigonal prismatic ones and in sec. III B we study the Raman spectrum of the distorted 1T' phase. Finally, in sec. III C we study catalytic adsorption of Hydrogen and its effect on the structural and electronic properties of the different structures.

II. TECHNICAL DETAILS

The results reported in the present paper were obtained from first-principles density functional theory in the generalized gradient approximation¹⁹. The QUANTUM-ESPRESSO²⁰ package was used with norm-conserving pseudopotentials and a plane-waves cutoff energy of 90 Ry. Semicore states were included in the Mo pseudopotential. The Electronic structure calculations were performed by using a 24×24 , 12×24 , 12×12 electron-momentum grids for the 1T, 1T' and 1T'' phases, respectively. For the metallic 1T structure we use an Hermitian-Gaussian smearing of 0.01 Ryd. The phonon dispersion of the 1T phase was calculated by Fourier interpolating dynamical matrices calculated on a 8×8 phonon-momentum grid and on a 24×24 electron-momentum grid. The Raman intensity calculation for the 1T' phase was performed on a 8×16 electron-momentum grid. The phonon dispersion calculation for the 1T' structure was performed using a 4×4 phonon momentum grid.

III. RESULTS

A. Stability of octahedral phases

We first investigate the relative stability of 2H and 1T phases in Fig. 1. As expected, we find that the 1H MoS₂ phase is the most stable one, with a lower energy of 0.83 eV / Mo atom with respect to the 1T one. The electronic structure calculation of the 1T structure in Fig. 2 shows that this polytype is indeed metallic. Differently from the 1H case, here the spin-orbit coupling is very weak and from now on it will be neglected.

As the energy difference between the 1T and 2H phases is more then 30 times larger then the 200-300 K annealing temperature necessary to transform the 1T phase in the 2H one, the experimental detection of the 1T and 1T' phases cannot be inferred from the total energy difference between the two. It has been suggested that the 1T phase is metastable and, as a consequence, an energetic barrier occurs between the two⁹. To verify this hypothesis, we calculate the phonon dispersion for the 1T phase. We find that the 1T structure is dynamically unstable (see Fig. 3) at zone border, with the largest instability at the M point of the hexagonal lattice. This

Atom	x	y	z
Mo	0.0508948	0.0508948	0.0051972
S	0.1662841	0.6662835	0.1240922
S	0.3337158	0.3337161	-0.1240922
Mo	0.4491051	-0.0508948	-0.0051972
S	0.6714116	0.6714108	0.0957802
S	0.8285883	0.3285888	-0.0957802

TABLE I: Atomic coordinates with respect to the direct axis for the 1T' structure. The lengths of the two direct lattice vectors of the two dimensional lattice are identified by $a = 6.411\text{\AA}$, $b = 3.111\text{\AA}$. The angle between them $\gamma = 119.034^\circ$.

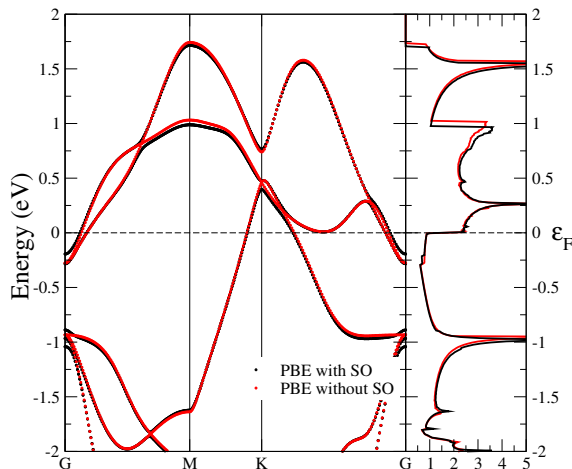


FIG. 2: Electronic structure and density of states of the 1TMoS₂ phase with or without spin orbit coupling. The energy are plotted with respect to the Fermi level.

distortion is compatible with a 2×1 superstructure. To identify the lowest energy superstructure, we perform calculations on a 2×1 supercell, by displacing the atoms along the direction given by the phonon displacement of the most unstable mode at M. We find that substantial energy (0.19 eV/ Mo) is gained by the distortion. We then start from this distorted structure and perform full structural optimization of internal coordinates and of the 2D-cell. As shown in Figs. 6, we find a stabilization of an octahedrally coordinated structure composed of zig-zag chains, with an energy gain of 0.29 eV/Mo with respect to the 1T phase. Structural parameters of the zig-zag distorted-structure are given in Tab. I. Here we remark that the shortest distance between Mo atoms belonging to the same chain is $\approx 2.72\text{\AA}$, while the shortest distance between atoms on different chains is $\approx 3.71\text{\AA}$. The angle between the Mo atoms in the chain is $\approx 69.64^\circ$. The in-plane nearest-neighbours Mo-Mo distance of the 1T' structure is almost identical to the nearest neighbours distance of Mo atoms in bcc Mo²¹, that is 2.728\AA . On the contrary in the 1T structure the Mo-Mo bonds is 3.193\AA , substantially elongated with respect to the Mo-Mo nearest neighbour distance in bcc Mo.

The devised 1T' structure closely resembles that detected in experiments on chemically exfoliated samples¹³.

The electronic density of states of the distorted structure is shown in Fig. 7. The distortion opens a very small gap (≈ 0.045 eV) that makes the system insulating. The formation of zig-zag chains is actually very similar to the standard Peierls dimerization in one dimensional systems, i. e. the system gains energy in opening

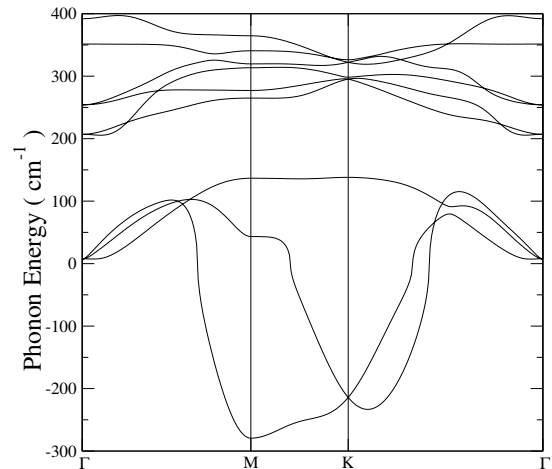


FIG. 3: Phonon dispersion of the 1TMoS₂ phase showing a dynamical instability at zone border.

a gap. The Peierls distortion reduces the dimensionality of the 2D layer that is now broken in 1D zig-zag chains. This is at odd with most bulk metallic transition metal dichalcogenides where the charge density wave state coexists with metallicity and superconductivity¹. However, given the large energy gain and the strong bond deformation involved in this distortion, the transition to 1D-zig-zag chains has to be considered more a real structural transition than a charge density wave.

Atom	x	y	z
Mo	0.022531337	0.022531337	0.0
S	0.317728127	0.651403657	0.056424736
S	0.651403657	0.317728127	-0.056424736
Mo	0.465000117	0.001783220	-0.000455305
S	0.815301793	0.651805630	0.049761398
S	1.150643861	0.316295157	-0.062393003
Mo	0.444399776	0.444399776	0.0
S	0.814643878	1.148463448	0.056499460
S	1.148463448	0.814643878	-0.056499460
Mo	0.001783220	0.465000117	0.000455305
S	0.316295157	1.150643861	0.062393003
S	0.651805630	0.815301793	-0.049761398

TABLE II: Coordinates of the 12 atoms in the 1T'' unit-cell with respect to the direct lattice vectors. The lengths of the two direct lattice vectors of the two dimensional lattice are identified by $a = b = 6.422\text{\AA}$. The angle between the two is $\gamma = 119.331^\circ$.

As the energy difference between the 1T' and the 1H structures is large (0.54 eV/Mo), we perform additional

<i>Theory</i> (cm^{-1})	<i>Theory</i> (Intensity)	<i>Experiment</i> ¹⁸ (cm^{-1})	1HMoS ₂ ¹⁷ (cm^{-1})
147	0.003		
151	0.008	156 (J1)	
216	1.0	226 (J2)	
223	0.006		
286	0.011	287	
333	0.033	333 (J3)	
350	<0.001	358	385 (E _{2g})
412	0.13	408	403 (A _{1g})

TABLE III: Calculated phonon frequencies (in cm^{-1}) and first-order Raman intensities of the 1T' phase, as compared with experiments on both 1T' and 1H phases. The intensities are normalized to the most intense peak. The incoming and outgoing light in the Raman experiment are assumed to be unpolarized. See Ref. 22 for more details on the definition of the Raman intensities.

structural optimization on the 2×2 supercell to see if other superstructures can be stabilized. We do indeed find another distorted structure formed by Mo rhombus (1T'' MoS₂, see Fig. 1 and Tab.II) that is 0.19 eV lower in energy than the 1T structure but still higher than both the 1T' and the 1H one. Interestingly, in past experimental works on chemically exfoliated MoS₂ samples⁶, a similar 1T'' structure was proposed as the most stable one in the monolayer.

B. Raman spectra of the distorted 1T' phase

In order to substantiate that the 1T' structure determined theoretically is the same of the experimental one, we calculate the phonon frequencies at zone center and the first-order Raman intensities for the 1T' structure. We also give a complete interpretation of Raman spectra in chemically exfoliated samples that is currently lacking in literature.

In 1H MoS₂, at high energy, only two Raman peaks are seen, namely the E_{2g} mode at $\approx 385 cm^{-1}$ and the A_{1g} mode at $\approx 403 cm^{-1}$ (see Ref. 17). The experimental Raman spectra of the 1T' phase show two main variations with respect to H-polytypes: (i) the E_{2g} peak disappears and (ii) five additional peaks occur (see Table III). Due to the reduced symmetry of the 1T' structure, we do indeed find several Raman active peaks and a very rich spectrum. The E_{2g} peak is missing and the additional calculated Raman peaks can be associated to the experimental ones with a high degree of accuracy.

In our calculation the peak with the largest intensity is the so called J₂ peak at $216 cm^{-1}$ ($226 cm^{-1}$ in experiment). This mode tends to shorten the distance between the two zig-zag chains and to recover the 1H structure (see Fig. 4). In experiments¹⁸ this mode has a much larger linewidth than all the others. This partly explains why the experimental height of the peak is substantially

reduced with respect to the Raman intensity.

The so called J₁ peak at $156 cm^{-1}$ in experiments is actually composed of two different phonon modes at $4 cm^{-1}$ distance one from the other. The one at $147 cm^{-1}$ shifts out-of-plane and in opposite directions each stripe of Mo atoms inside the zig-zag chain. The mode at $151 cm^{-1}$ is an in-plane shearing mode of one stripe of atom with respect to the other inside a chain. The peaks at $233 cm^{-1}$ and at $286 cm^{-1}$ involve shifts of the S-atom layers with respect to the Mo atoms. The J₃ mode at $333 cm^{-1}$, in excellent agreement with experiments, tends to break each zig-zag chain in two stripes with a slight out-of-plane component. The mode at $350 cm^{-1}$ compares favourably with the $358 cm^{-1}$ peak detected in experiments, although in theory it has a too small intensity. Finally, the mode at $412 cm^{-1}$ is nothing else than the usual A_{1g} mode seen in the 1H polytype. The agreement between the calculated zone-center energies and the position of Raman peaks suggests that the devised structure closely resembles the experimental one. Some disagreement still exists between the calculated relative intensities and the experimental ones. However, it should be noted that Raman spectra on different samples^{14,18} show substantially different Raman intensities, probably due either to the inhomogeneity of the sample composed of several phases or to the presence of adsorbates and vacancies.

Finally in Fig. 5 we show the calculated phonon dispersion of the 1T' structure that is dynamically stable, suggesting that an energy barrier does indeed exist between the 1H and the 1T' phases and that the 1T' is metastable.

C. Catalytic adsorption

In order to justify the stabilization of the 1T' crystal structure with respect to the 1H one detected in experiments, we study adsorbates adsorption on the 1H, 1T, 1T' and 1T'' phases. Single layers MoS₂ samples at the end of the chemical exfoliation process are fully covered with adsorbates, due to the hydration of Li_xMoS₂ with water. We focus on the simple case of H adsorption. We consider 4×4 supercells of the 1T and 2H phase, as well as 2×4 supercells of the 1T' unit cell. We start considering only one H ion at random positions on top of the MoS₂ layer and then perform several structural optimizations. We find that the H ion always binds to an S-atom, similarly to what happens in WS₂⁹. Indeed, in the absence of adsorbates, a positive (negative) charge resides on the Mo (S)-atom²³, as it can also be inferred from the relative electronegativity of S and Mo. We then add a second H atom and find that two H atoms prefer to bind to different S atoms. Thus, we consider as starting guess of the structural minimization all the possible ways of binding H to different S atoms that are compatible with the supercell size.

By performing structural minimization, we find that

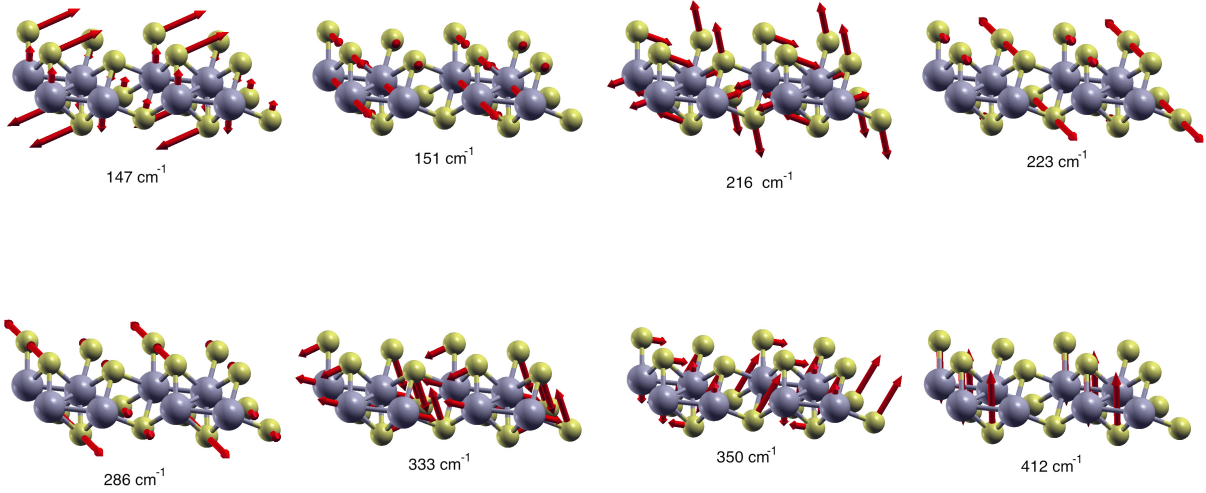


FIG. 4: Raman active modes of $1T'$ MoS_2 single-layer. The length of the arrows is proportional to the modulus of the phonon eigenvector.

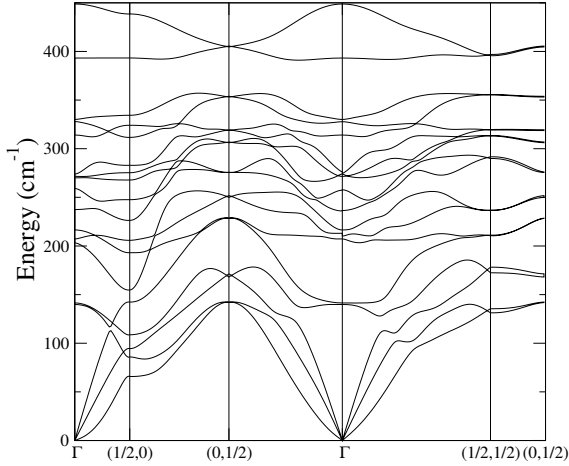


FIG. 5: Phonon dispersion of the $1T'$ structure along selected directions

at all H coverages the 1H structure retains its trigonal prismatic coordination. Similarly, even when higher in energy, the H-covered $1T'$ structure never decays into the 1H one, but preserves its zig-zag structure, although the separation between the chains and the bonding inside the chain are affected by H concentration. This confirms once more that an energy barrier does indeed occur between the 1H and the $1T'$ structures. Finally, we find that the

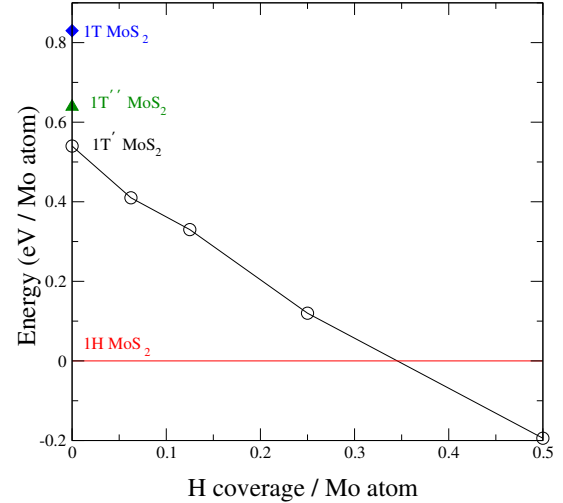


FIG. 6: Stability of different MoS_2 structures with respect to the 1H polytype and as a function of H coverage per Mo atom

H-covered 1T structure always decays into the H-covered $1T'$ one, confirming the dynamical instability of the 1T phase towards the $1T'$. At large enough coverage, this is also what happens to the $1T'$ structure that also decays on the $1T'$.

In Fig. 6 we show the lowest energy configuration of all phases with respect to the most stable configuration of the 1H structure at a given H-coverage. We find that at

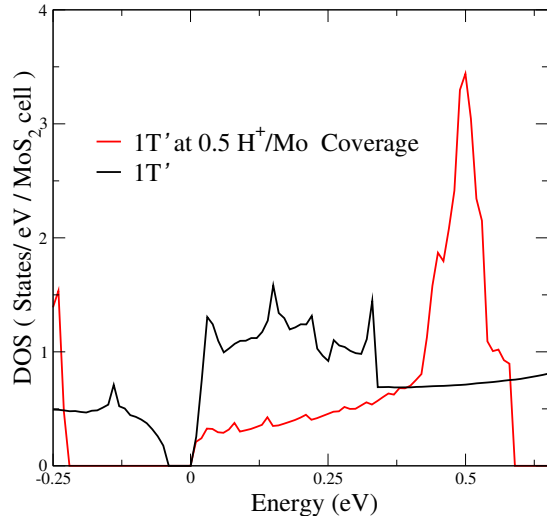


FIG. 7: Electronic density of states of the $1T'$ at 0 and 0.5 H/Mo coverage. The zero of the energy has been set to the bottom of the conduction band.

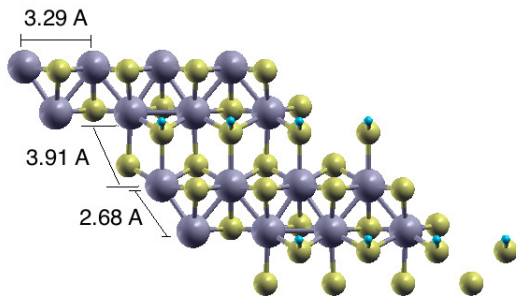


FIG. 8: Most stable structure at 0.5 H coverage (left). The S atoms are depicted in yellow, while the hydrogens are the small cyan spheres.

H coverages superior to 0.35 / Mo, the $1T'$ phase is more stable than the $1H$ one. This suggests that in chemically exfoliated MoS_2 monolayers, the samples are divided in H-rich regions where the $1T'$ structure is stabilized and in H-poor regions where the $1H$ phase is stabilized.

By comparing in details the $1T'$ structures at 0 and 0.5 H/Mo coverage (see Fig. 8), it is seen that upon H adsorption the separation between the chains strongly increases, as the shortest distance between Mo atoms on different chains is 3.91 Å (3.71 Å) at coverage 0 H/Mo (0.5 H/Mo). Furthermore at coverage 0.5 H/Mo the Mo atoms do not lay on the same plane, as in the undistorted case, but are displaced above or below by ≈ 0.07 Å. The increased distance between the chains implies a larger band gap and more insulating character, as shown in Fig.

7. This agrees with experiments where it was found that the zig-zag chain structure is indeed insulating^{13,14}.

IV. CONCLUSION

Chemically and mechanically exfoliated MoS_2 single-layer samples have substantially different properties. While mechanically exfoliated single-layers are mono-phase ($1H$ phase), the chemically exfoliated samples show coexistence of three phases, $1H$, $1T$ and $1T'$. The fact that three phases experimentally coexist could lead to the conclusion that the three pure structures have similar energies. However, as we have shown in the present work, this is far from being the case, as all octahedrally coordinated phases are much higher (more than 0.54 eV/Mo) in energy than the trigonal prismatic one ($1H$). Moreover, the pure (i.e. without adsorbates or vacancies) $1T$ phase is dynamically unstable and undergoes a phase transition, again with a considerable energy gain (0.29 eV / Mo), towards the most stable $1T'$ structure composed of separated zig-zag chains. This finding strongly questions the detection of the pure $1T$ phase in experiments^{13,14,16} and points to a key role of either adsorbates or vacancies in stabilizing the $1T$ metallic structure.

We have calculated dynamical properties of the lowest energy octahedral structure ($1T'$) and found that it is dynamically stable, suggesting that an energy barrier does indeed exist between the $1H$ and the $1T'$, similar to what happens in WS_2 where nudged elastic band calculations²⁴ find a 0.92 eV/Mo barrier between the $1T'$ and the $1H$ phases. By investigating catalytic adsorption on single-layer MoS_2 we demonstrate the key role of adsorbates, and, more generally, of negative charging of the MoS_2 layer, in stabilizing the $1T'$ phase. This phase becomes the most stable at concentrations of ≈ 0.35 H / Mo.

Finally, we provided a microscopical description of the $1T'$ Raman spectrum attributing the J_1 , J_2 and J_3 features to specific vibrations. These features were experimentally detected in 1986⁴, but their interpretation and understanding was unknown.

Our work represents the first complete study of static and lattice dynamical properties of chemically exfoliated samples. We believe that our results will be of great interest for future studies of chemically exfoliated two dimensional crystals.

V. ACKNOWLEDGEMENTS

The author acknowledges useful discussions with Manish Chhowalla and Goki Eda. The author acknowledges support from the Graphene Flagship and from the French state funds managed by the ANR within the Investissements d'Avenir programme under reference ANR-11-IDEX-0004-02, ANR-11-BS04-0019 and ANR-13-IS10-0003-01. Computer facilities were provided by

CINES, CCRT and IDRIS (project no. x2014091202).

-
- * matteo.calandra@upmc.fr
- ¹ Wilson J. A., Di Salvo F. J. and Mahajan S. , *Advances in Physics*, **24**, 117 (1975)
 - ² J. T. Ye, Y. J. Zhang, R. Akashi, M. S. Bahramy, R. Arita and Y. Iwasa, *Science* **30**, 1193 (2012)
 - ³ Frindt, R. F. , *J. Appl. Phys.* **37**, 1928 (1966)
 - ⁴ Joensen, P.; Frindt, R. F.; Morrison, S. R. n *Mater. Res. Bull.* **21**, 457 (1986)
 - ⁵ Frindt, R. F. , *Phys. Rev. Lett.*, **28**, 299 (1972)
 - ⁶ Yang, D.; Sandoval, S. J.; Divigalpitiya, W. M. R.; Irwin, J. C.; Frindt, R. F. , *Phys. Rev. B*, **43**, 12053, (1991).
 - ⁷ Novoselov K. S., Jiang D., Schedin F., Booth T. J., Khotkevich V. V., Morozov S. V. and Geim A. K., *PNAS* **102**, 1045110453 (2005)
 - ⁸ Coleman, JN; Lotya, M; O'Neill, A et. al., *Science*, **331** 568-571 (2011)
 - ⁹ Chhowalla, M, Shin, H. S., Eda, G., Li, L. J., Loh, K. P., and Zhang H.,*Nature Chemistry* **5**, 263-275 (2013)
 - ¹⁰ Radisavljevic B., Radenovic A., Brivio J., Giacometti V., and A. Kis, *Nature Nanotechnology* **6**, 147 (2011)
 - ¹¹ Furer M. S. and Hone J., *Nature Nanotechnology* 2013, **8**, 146147, Kis A. and Radisavljevic B., *Nature Nanotech.*, **8**, 147 (2013)
 - ¹² *Graphene is not alone*, *Nature Nanotechnology*, **7**, 683 (2012)
 - ¹³ Eda G., Fujita, T., Yamaguchi H., Voiry D., Chen M., and Chhowalla M., *ACS Nano*, **6** 7311 (2012)
 - ¹⁴ Eda G., Yamaguchi H., Voiry D., Fujita T., Chen M., and Chhowalla M., *Nano Lett.* **11**, 5111-5116 (2011)
 - ¹⁵ Komsa H. P., Kotakoski J., Kurasch S., Lehtinen O., Kaiser U., Krasheninnikov A. V., *PRL* **109**, 035503 (2012)
 - ¹⁶ Yung-Chang Lin, Dumitru O. Dumcenco, Ying-Sheng Huang, Kazu Suenaga., arXiv:1310.2363
 - ¹⁷ Lee C., Yan H., Brus L. E., Heinz T. F., Hone J., and Ryu S., *ACS Nano*, **4** 2695, (2010)
 - ¹⁸ Sandoval S. J., Yang D., Frindt R. F., and Irwin J. C., *Phys. Rev. B* **44**, 3955, (1991)
 - ¹⁹ Perdew J. P. , Burke K., Ernzerhof M., *Phys. Rev. Lett.* **77**, 3865 (1996) Unused bibitems
 - ²⁰ P. Giannozzi *et al.*, *J. Phys. Condens. Matter* **21**, 395502 (2009).
 - ²¹ N. Ashcroft and N. D. Mermin, *Solid state physics*, Harcourt College Publishers, 1976
 - ²² Boukhicha M., Calandra M., Measson M. A., Lancry O., and Shukla A., *Phys. Rev. B* **87**, 195316 (2013)
 - ²³ Ataca C. and Ciraci S., *Phys. Rev. B* **85**, 195410 (2012)
 - ²⁴ Voiry, Yamaguchi D. H., Li J., Silva R., Alves D. C. B., Fujita T., Chen M. , Asefa T., Shenoy V. B., Eda G., and Chhowalla M., *Nature Materials*, **12** , 850 (2013)